Acta Neurochirurgica (2019) 161:1535–1543
https://doi.org/10.1007/s00701-019-03911-7

ORIGINAL ARTICLE - NEUROSURGICAL ANATOMY

The approach angle to the interoptic triangle limits surgical workspace when targeting the contralateral internal carotid artery

Lucas Ezequiel Serrano[1] · Eleftherios Archavlis[1] · Ali Ayyad[2] · Amr Nimer[3] · Eike Schwandt[1] · Florian Ringel[1] · Sven Rainer Kantelhardt[1]

Received: 25 February 2019 / Accepted: 10 April 2019 / Published online: 18 May 2019

Abstract

Background The interoptic triangle (IOT) offers a key access to the contralateral carotid artery's ophthalmic segment (oICA) and its perforating branches (PB), the ophthalmic artery (OA), and the superior hypophyseal artery (SHA). It has been previously reported that the assessment of IOT's size is relevant when attempting approaches to the contralateral oICA. However, previous studies have overseen that, since the oICA is a paramedian structure and a lateralized contralateral approach trajectory is then required, the real access to the oICA is further limited by the approach angle adopted by the surgeon with respect to the IOT's plane. For this reason, we determined the surgical accessibility to the contralateral oICA and its branches though the IOT by characterizing the morphometry of this triangle relative to the optimal contralateral approach angle.

Methods We defined the "relative interoptic triangle" (rIOT) as the two-dimensional projection of the IOT to the surgeon's view, when the microscope has been positioned with a certain angle with respect to the midline to allow the maximal contralateral oICA visualization. We correlated the surface of the rIOT to the visualization of oICA, OA, SHA, and PBs on 8 cadavers and 10 clinical datasets, using for the last a 3D-virtual reality system.

Results A larger rIOT correlated positively with the exposure of the contralateral oICA ($R = 0.967$, $p < 0.001$), OA ($R = 0.92$, $p < 0.001$), SHA ($R = 0.917$, $p < 0.001$), and the number of perforant vessels of the oICA visible ($R = 0.862$, $p < 0.001$). The exposed length of oICA, OA, SHA, and number PB observed increased as rIOT's surface enlarged. The correlation patterns observed by virtual 3D-planning matched the anatomical findings closely.

Conclusions The exposure of contralateral oICA, OA, SHA, and PB directly correlates to rIOT's surface. Therefore, preoperative assessment of rIOT's surface is helpful when considering contralateral approaches to the oICA. A virtual 3D planning tool greatly facilitates this assessment.

Keywords Contralateral approach · Internal carotid · Interoptic triangle

Introduction

The close anatomic relation of clinoid and ophthalmic segments of the internal carotid artery (oICA) and its branches, to the optic apparatus, cavernous sinus, and surrounding bone, render the surgical treatment of aneurysms in this area difficult [7, 8, 10, 12, 16, 19, 21, 22].

Since most of oICA aneurysms arise and point medially, conventional ipsilateral pterional and orbitozygomatic approaches usually require significant ICA and optic nerve mobilization, as well as anterior clinoidectomy. These procedures are, however, associated with a specific surgical risk and morbidity [1, 3, 25, 33]. Contralateral approaches could provide better exposure of the oICA's superomedial aspect, the ophthalmic-(OA) and superior hypophyseal arteries (SHA),

This article is part of the Topical Collection on *Neurosurgical Anatomy*

✉ Lucas Ezequiel Serrano
lucas.serrano@unimedizin-mainz.de

[1] Department of Neurosurgery, Mainz University Medical Center, Langenbeckstraße 1, 55131 Mainz, Germany

[2] Department of Neurosurgery, Saarland University Hospital, Kirrbergerstraße 100, 66421 Homburg, Germany

[3] Department of Neurosurgery, Charing Cross Hospital, Imperial College Healthcare, Fulham Palace Rd, London W6 8RF, UK

sparing the need of anterior clinoidectomy and minimizing ICA and ON retraction [8, 9, 20, 21, 28–31]. The access to the contralateral oICA is given by an approach route passing through the interoptic triangle (IOT), formed by both optic nerves and the bone of the skull base between both optic foramina, with its apex formed by the optic chiasm. Several authors mention the importance of the actual size of the interoptic space, respectively, the IOT, when approaching the contralateral oICA [14, 23]. Considering that the oICA is a paramedian structure, the surgical space to access the contralateral oICA is, however, further limited as the IOT is approached via a certain angle (see Fig. 1). Yet, no systematic morphometric study has investigated the exact surgical workspace across the IOT when operating from a lateralized approach.

To get a clearer idea of the actual practical surgical workspace, we defined the "relative interoptic triangle" (rIOT) as the two-dimensional projection of the IOT to the surgeon's view, when the microscope has been positioned with a certain angle with respect to the midline to allow the maximal contralateral oICA visualization behind the IOT (see schematic representation on Fig. 1). In the present study, we investigated this rIOT in cadaver specimens and in virtual 3D workspace based on MRI and CT data of individual patients. The latter was performed to adapt for moderate changes in vasculature morphology that can occur during cadaveric conservation [27]. Besides this, we evaluate whether a 3D planning tool can be helpful to assess the surgical space in individual cases and might be helpful during planning of an optimal approach on an individual basis.

Materials and methods

Anatomical study in cadaveric specimens

All cadaveric dissections were performed in an experimental microsurgical research laboratory at our institution. Eight adult heads conserved in a formaldehyde solution of 40 g/L were used to perform 16 craniotomies. All ethical and hygienic procedures followed the standards ruled by the Hygiene and Health Department of our institution and current national and international standards. Craniometric measurements on the sagittal, coronal, and axial planes were performed for each head to rule out major anthropometric differences between specimens and asymmetries between hemispheres.

Each specimen was subjected to bilateral classical pterional (frontotemporosphenoidal) craniotomies and microsurgical dissections directed to the oICA following a systematic manner [33].

Heads were mounted in a 19 × 19-cm quadrangular holder and fixed in 4 points with adjustable pins in supine position. Positioning resembled standard pterional craniotomies, directed about 20° vertex down, elevated slightly, and rotated about

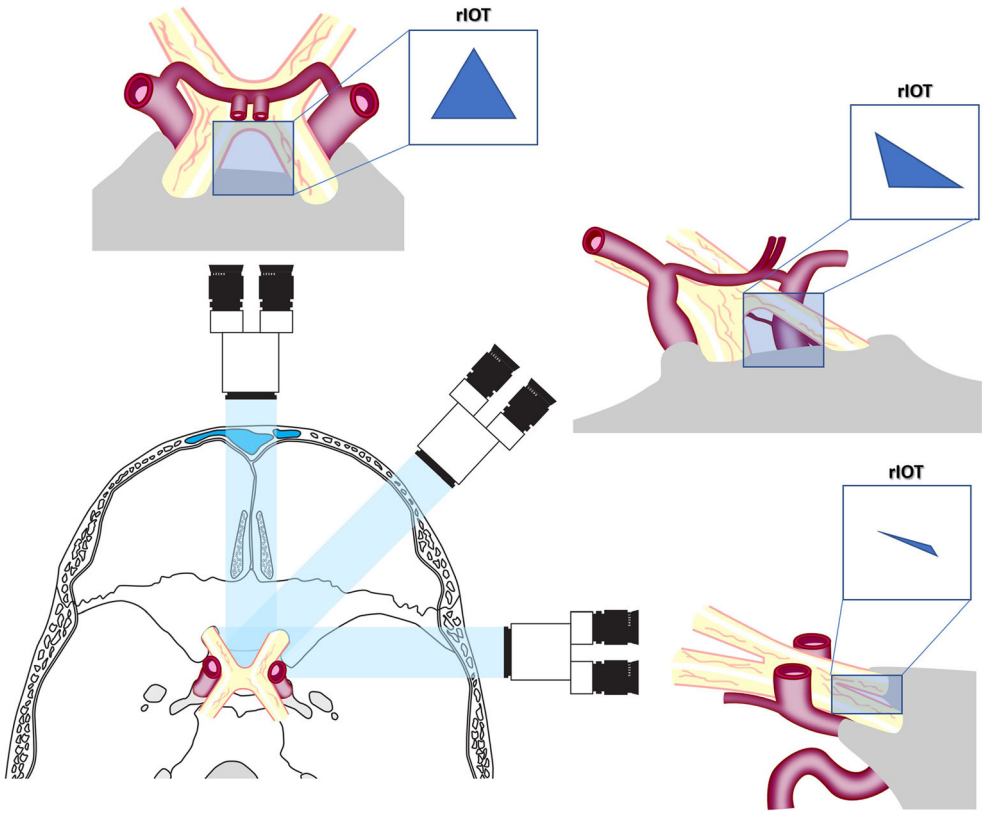

Fig. 1 Schematic representation of the relative interoptic triangle (rIOT). The triangular space between both optic nerves in their intracranial course acquires a different two-dimentional projection in terms of shape and surface to microscopic's view according to the axial angle of approach. This was defined as the relative interoptic triangle (rIOT). Theoretically, if the view is orthogonal to interoptic triangle's axis, the two-dimentional workspace, i.e., rIOT (**a**), differs significantly in shape and projected apparent surface from the one when the trajectory is tangential to interoptic triangle's axis (**c**). To approach the medial wall of the contralateral oICA, a subfrontal trajectory is needed and the two-dimentional projection of the interoptic triangle to surgeon's view differs according to the approach angle adopted (**b**)

45° to bring the malar eminence to the uppermost point of the operating field. Craniotomies were extended anteriorly above the orbital roof up to the supraorbital foramen, as well as posteriorly up to 4 cm along the temporal squama. After elevating the bone flap, the temporal squama and greater wing of the sphenoid bone were rongeured toward the floor of the middle fossa, allowing greater mobilization of the anterior temporal lobe. The rough bone of the posterolateral orbital roof was smoothed and the posterior ridge of the lesser wing of the sphenoid bone was progressively flattened until the orbital-meningeal fold was reached.

Further dissection was carried out intradurally towards the anterior parasellar region. The approaches were directed through a corridor above the orbital roof allowing frontal lobe retraction up to a maximum of 15 mm (subfrontal/supraorbital route).

In the depth the optic chiasm, both optic nerves, contralateral oICA including its perforating branches, as well as contralateral ophthalmic- (OA) and superior hypophyseal arteries (SHA) were exposed (Fig. 2) and the falciform fold was opened above both optic nerves. Now, the microscope angulation was adapted to get the approach trajectory that allowed the maximal visualization of the contralateral oICA through the IOT. At this point, the rIOT (two-dimentional projection of the IOT to microscope's view) and the contralateral vascular structures were morphometrical characterized after each of the following steps: (i) prior to removal of any bone; (ii) after ipsilateral intradural anterior clinoidectomy and opening of the falciform ligament; (iii) after removing the contralateral half of the planum sphenoidale and tuberculum sellae; (iiii) prior and after mobilization of the contralateral optic nerve.

Morphometric characterization included measurement of the rIOT's surface (applying the formula base × height/2), counting the number of perforating branches of the oICA and determining the exposed length of oICA, OA, and SHA.

Simulation of surgical approaches in a virtual 3D workspace base on individual patient data

To perform virtual 3D simulations, we randomly selected preoperative cranial image sets of 10 patients. Simulation was performed using the 3D-imaging-tool dextroscope® (Volume Interactions Pte. Ltd.). Data acquisition and image processing in the virtual workspace using the dextroscope® are described in detail by Kockro et al. [17].

Virtual dissection and assessment followed the identical stepwise pattern as cadaveric dissection. Using the handheld pen-eraser-tool, we removed skin and temporal muscle. This was followed by a virtual craniotomy using the same anatomical landmarks as for cadaveric specimens. Since brain retraction is not feasible in the Dextroscope®, it was simulated by virtually erasing a 15-mm layer of brain parenchyma.

By virtual dissection, the same structures were exposed as during cadaveric dissection, namely the contralateral oICA, ipsi- and contralateral optic nerves, the optic chiasm and contralateral OA. Due to resolution limitations, finer structures, such as the SHA and tiny perforant branches, could not be segmented.

Corresponding to cadaveric dissection, virtual morphometric characterization of the rIOT surface as well as previously listed neurovascular structures was performed (Fig. 3). Since bending of structures is not feasible using the dextroscope®, characterization of contralateral vascular elements could be assessed prior to optic nerve mobilization only.

Statistical analysis

For each variable, we performed a Shapiro-Wilk goodness of fit test to determine its parametric or non-parametric distribution. In the case of normal distribution, we expressed the central tendency measure as the arithmetic mean and its dispersion as standard deviation. For variables following non-parametric distributions, the central tendency measure was expressed as the median of the sample and its dispersion as interquartile ranges.

For comparison the means of two or more than two normal distributed variables we used ANOVA. The effect size for significant p values was expressed as partial eta square (η_p^2) values. For variables following non-parametric distributions, we used the Mann-Whitney-Wilcoxon U test to assess significance. Statistical significance was assumed if the p value was found > 0.05. For correlation analysis, we performed scatter plots and calculated Pearson's r correlation coefficient.

Finally, to set our alpha levels, post hoc Bonferroni corrections were performed. For statistical work, we used the software package IBM SPSS Statistics v23.

Results

Morphometric analysis of the relative interoptic triangle in cadaveric specimens

The mean surface of the rIOT seen during contralateral approaches directed through an optimized subfrontal/supraorbital angle was 81.19 ± 9.52 mm^2. As expected, an ipsilateral anterior clinoidectomy did not modify these morphometric parameters. Bone removal of the planum sphenoidale and tuberculum sellae increased the surface of rIOT significantly to 98.12 ± 11.15 mm^2 [$F(1, 31) = 21{,}355$, $p < 0.001$, $\eta_p^2 = 0.416$]. Optic nerve mobilization increased the surface of the interoptic triangle to 107.5 ± 10.69 mm^2 [$F(1, 31) = 54{,}047$, $p < 0.001$, $\eta_p^2 = 0.643$]. A comparison of the rIOT's surface following planum sphenoidale removal and following optic nerve mobilization resulted in a significantly

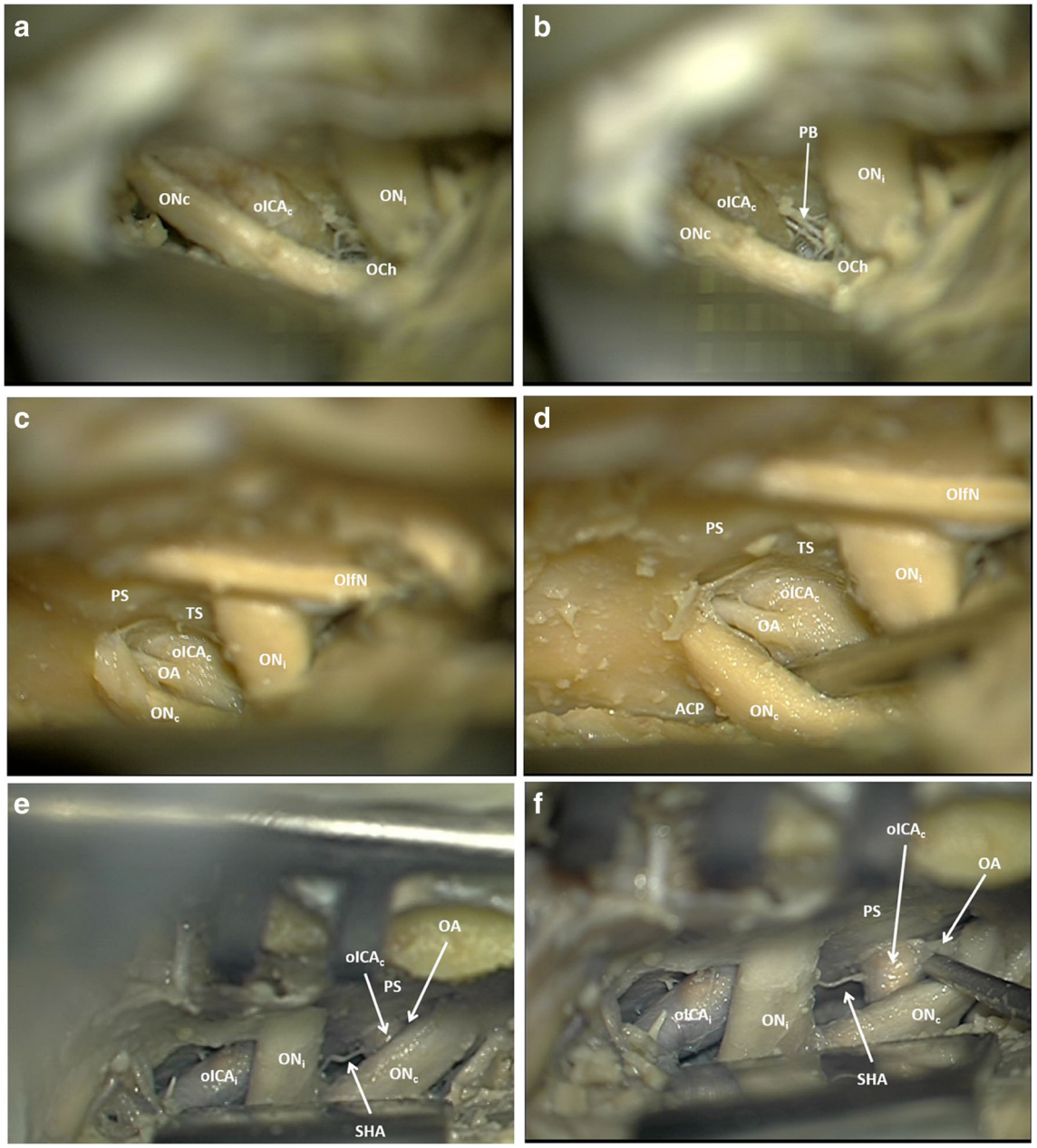

Fig. 2 Representative rIOT dissections in different cadaveric specimens. A pterional craniotomy was performed and the interoptic space was reached by following a route below the frontal lobe. The rIOT, limited by the optic chiasm, the intracranial course of both optic nerves and the chiasmatic groove, enabled a successful exposure of the medial aspect of the contralateral internal carotid artery as well as the superior hypophyseal and ophthalmic arteries. *ACP*, anterior clinoid process; *OlfN*, olfactory nerve; *FL*, falciform dural fold (ligament); *ON$_i$*, ipsilateral optic nerve; *ON$_c$*, contralateral optic nerve; *Och*, optic chiasm; *oICA$_c$*, ophthalmic segment of the contralateral internal carotid artery; *oICA$_i$*, ophthalmic segment of the ipsilateral internal carotid artery; *OA*, contralateral ophthalmic artery; *SHA*, contralateral superior hypophyseal artery; *PB*, perforant branches of the oICA; *PS*, planum sphenoidale; *TS*, tuberculum sellae

greater surface following the second maneuver [$F(2, 47) = 22{,}102$, $p < 0.001$, $\eta_p^2 = 0.496$]. A combination of both, optic nerve mobilization and planum sphenoidale removal, further significantly increased the rIOT surface to 124.44 ± 12.15 mm^2 [$F(1, 31) = 5896$, $p < 0.01$, $\eta_p^2 = 0.164$] (Fig. 4).

A larger rIOT correlated positively with the exposure of the contralateral oICA ($R = 0.967$, $p < 0.001$), OA ($R = 0.92$, $p < 0.001$), SHA ($R = 0.917$, $p < 0.001$,) and the number of perforant vessels of the oICA visible ($R = 0.862$, $p < 0.001$) (Fig. 5). The exposed length of oICA increased from 6.2 ± 0.44 mm for specimens with rIOTs smaller than 75 mm^2 to 7 ± 0.1 mm for rIOTs between 75 and 85 mm^2 and 8 ± 0.1 mm for rIOTs larger than 85 mm^2. The same found for the exposed OA length (< 75 mm^2: 0.4 ± 0.89 mm; 75–85 mm^2: 1.66 ±

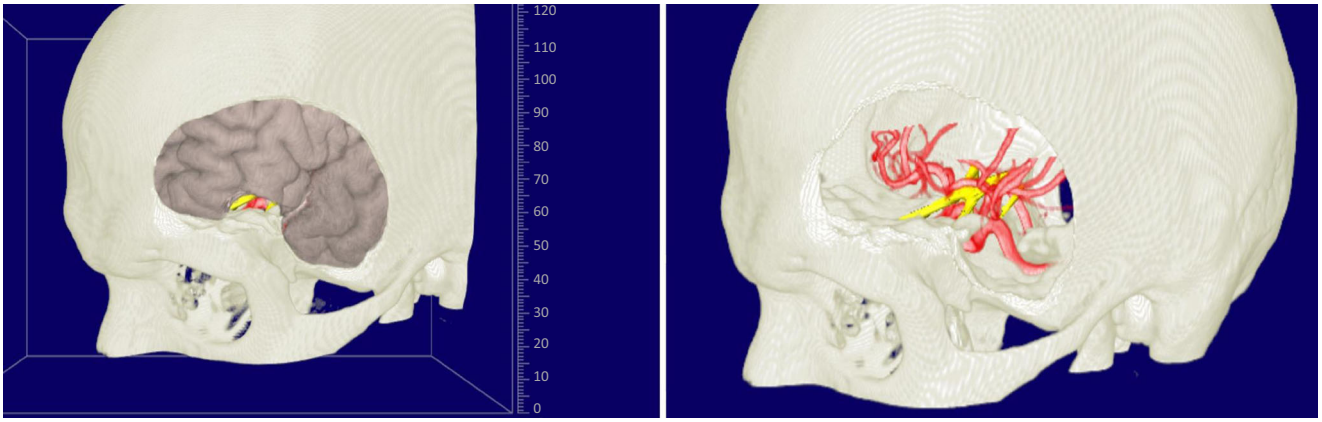

Fig. 3 Morphological characterization of the rIOT in living patients using a 3D simulation system. A pterional approach was performed and gentle frontal lobe retraction was simulated by erasing a layer of brain parenchyma corresponding to the inferior frontal gyrus and orbital gyri. Once the interoptic space was reached, a systematic morphometrical characterization of the rIOT, the contralateral internal carotid artery and the ophthalmic artery was accomplished

0.57 mm; > 85 mm^2: 2.87 ± 0.35 mm) and exposed SHA length (< 75 mm^2: 0 mm; 75–85 mm^2: 1.33 ± 1.15 mm; > 85 mm^2: 2.62 ± 0.51 mm). While rIOTs < 75 mm^2 allowed the visualization of two perforant branches from the oICA in 40% and three in 60% of the cases, rin IOTs > 85 mm^2 three perforant branches were observed in 87% and four in 13% of the cases. Further, we found that in specimens in which the origin of the OA and SHA could be visualized, rIOTs were significantly greater than in those where these structures remained covered ($p < 0.001$).

Relative interoptic triangle's assessment in a virtual 3D workspace based on individual patient data

The mean rIOT seen from optimized craniotomy sites using a subfrontal/supraorbital trajectory to the contralateral oICA was found to be 80 ± 8.59 mm^2. Removal of the ipsilateral anterior clinoid process did not influence these values. Removal of the contralateral half of the planum sphenoidale and tuberculum sellae significantly increased the rIOT to 90.2 ± 10.5 mm^2, as shown in separate one-way ANOVA [$F(2, 57) = 8.063$, $p = 0.001$] (Fig. 6).

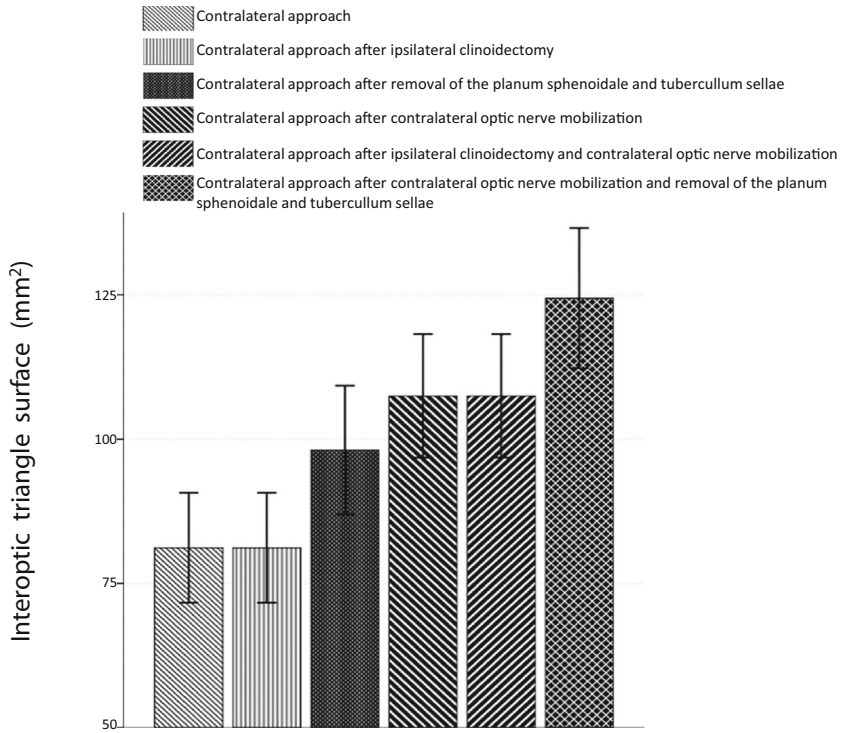

Fig. 4 Extension of the relative interoptic triangle surface for contralateral approaches in cadaveric specimens. All values express mean ± 2 SD

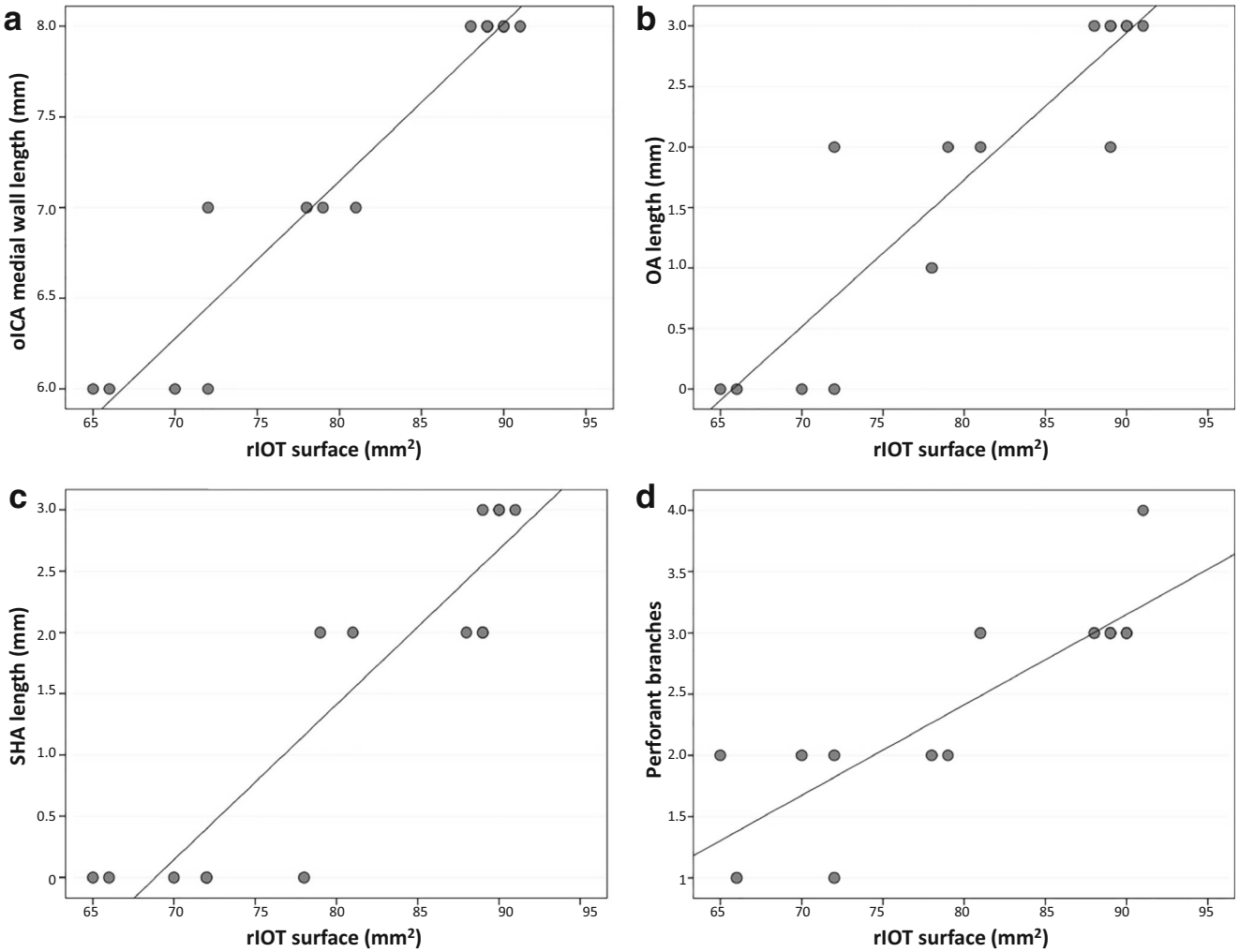

Fig. 5 Scatter plots showing correlation patterns between relative interoptic triangle (rIOT) extension and the extent of exposure of the contralateral oICA's medial wall (**a**), ophthalmic artery (**b**), superior hypophyseal artery (**c**), and perforant branches of the oICA (**d**) before removal of the contralateral half of the planum sphenoidale and tuberculum sellae as well as prior to contralateral optic nerve mobilization

Corresponding to the cadaveric dissections, virtual measurements revealed a strong positive correlation between the rIOT size and oICA and OA exposure (both $R = 0.915$, $p < 0.001$) (Fig. 6). This significant correlation remained after removal of the contralateral half of the planum sphenoidale and tuberculum sellae for both oICA ($R = 0.873$, $p < 0.001$) and OA exposure ($R = 0.955$, $p < 0.001$). The exposed length of oICA increased from 5.4 ± 0.55 mm for specimens with rIOTs smaller than 75 mm^2 to 6 ± 0.11 mm for rIOTs between 75 and 85 mm^2 and 6.87 ± 0.35 mm for rIOTs larger than 85 mm^2. The same was observed for the OA length (< 75 mm^2: 0 mm; 75–85 mm^2: 0.8 ± 0.48 mm; > 85 mm^2: 2.25 ± 0.46 mm). While rIOTs < 75 mm^2 allowed no visualization of OA origin, rIOTs between 75 and 85 mm^2 allowed visualization of the OA origin 28% of the cases, increasing to 87% in rIOTs > 85 mm^2. Additionally, virtual cases in which the OA origin could be visualized had a significantly greater rIOT both prior and after removal of the planum sphenoidale and tuberculum sellae (both $p < 0.001$).

Discussion

The interoptic space defines the way to access the oICA when using a contralateral approach. Therefore, the assessment of the interoptic space is crucial when planning an optimal approach to the oICA [9, 14, 23, 32]. Most commonly, the chiasm, and thus the apex of the interoptic triangle overlie the diaphragma sellae and the pituitary gland, a prefixed chiasm is situated over the tuberculum and a postfixed chiasm over the dorsum sellae. According to older anatomic studies, in approximately 70% of the cases, the chiasm is in the normal position and approximately the half of the remaining 30% are in prefixed, respectively, postfixed position [24]. All of

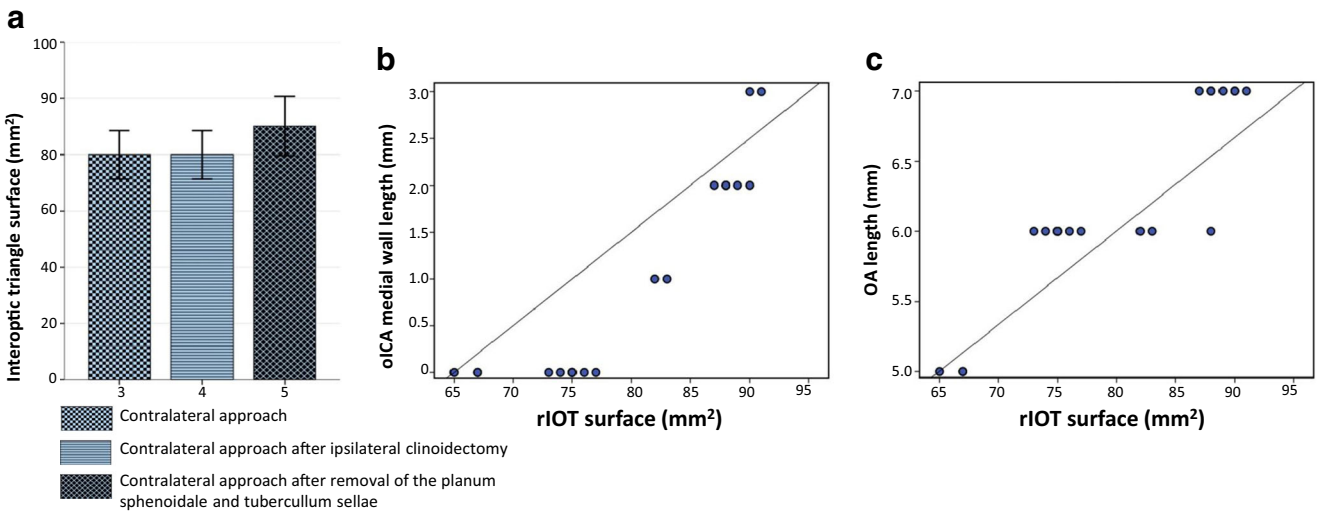

Fig. 6 Extension of the relative interoptic triangle's surface for contralateral approaches in 3D virtual dissections (**a**), as well as scatter plots obtained from 3D virtual dissections showing correlation patterns between relative interoptic triangle (rIOT) extension and the extent of exposure of the contralateral oICA's medial wall (**b**) and OA length (**c**) previous to the removal of the contralateral half of the planum sphenoidale and tuberculum sellae

our eight cadaveric specimens and ten virtual datasets presented a normal position of the chiasm.

Although the importance of the interoptic space as determinant for the accessibility to the contralateral oICA has been remarked previously, these studies have not considered that the approach angle to the contralateral oICA is not orthogonal as only seen from strictly anterior views [14, 23]. Given that the oICA is a paramedian structure, approaches to maximize its visualization are lateralized, a fact that further limits the workspace available to the surgeon (Fig. 1). Hence, we defined the rIOT to take into account this limitation. Further, this consideration allows to use the rIOT size and its position in relation to the targeted structure to optimize the craniotomy site. The area of this rIOT (orthogonal to the surgeon's view) significantly correlated to the exposure of the contralateral oICA and related structures. These findings confirm the previously reported surgical experience that sufficient interoptic space is required for the treatment of ICA pathology using a contralateral approach [6, 23]. The opening of the falciform ligament above the contralateral optic nerve is a further indispensable step when manipulating the contralateral ICA, the OA, and the optic nerve. It helps to avoid optic nerve injury from the sharp edge of this fold if the nerve is displaced superiorly and laterally [6, 23].

Furthermore, anatomical variances in this area render it advisable to evaluate the individual anatomy preoperatively. Virtual 3D simulation used in this study greatly facilitated this assessment and helped to determine the optimal craniotomy site.

Finally, removal of the contralateral half of the planum sphenoidale and contralateral optic nerve mobilization increased the rIOT, which significantly correlated to an increased exposure of the contralateral oICA and its branches. Nevertheless, these maneuvers must be carefully weighed against the additional risks implicate. Attempting bone removal with the power drill in this region can lead to mechanical or thermal injury on the optic nerve or the involved vessels; opening of the sphenoidal sinus increases the risk of CSF fistula. Similar considerations apply to mobilization of the contralateral optic nerve and several authors advised to avoid this maneuver if possible [2, 4, 6, 9, 11, 23]. While visual impairment due to optic nerve mobilization constitutes a serious concern in ipsilateral approaches to the oICA [15, 18, 26, 34], an advantage provided by contralateral approaches is that optic nerve mobilization is drastically reduced and often not even required to sufficiently expose the ICAs medial wall and its main branches [5, 6, 13, 18, 23, 30].

Conclusions

When approaching the contralateral ICA and surrounding structures, the triangle formed by the optic nerves and skull base limit the surgical workspace. If this interoptic triangle is not exposed from a strictly anterior view, as in most surgical cases where lateralized craniotomies are needed, the space is further limited by the angulation under which the triangle is approached. Therefore, we defined and assessed the size of the interoptic triangle as seen from the surgeon's perspective (relative interoptic triangle resp. rIOT). By cadaveric dissection and virtual 3D simulation, we could show that the exposure of contralateral oICA, OA, SHA, and PB directly correlates to the actual size of this rIOT. Further virtual 3D simulation might be helpful to assess accessibility and to optimize the

craniotomy site when considering a contralateral approach to the oICA.

Acknowledgements We want to thank very much Mr. Thomas Bauer for assistance with drawings for the Fig. 1, which greatly improved the intended message of our manuscript.

Compliance with ethical standards

Conflict of interest The authors declare that they have no conflict of interest.

Ethical approval This article does not contain any studies with human participants or animals performed by any of the authors. The cadaveric study followed all ethical and hygienic procedures ruled by the Hygiene and Health Department of our institution and current national and international standards. Ethical committee approval was not required as presented data correspond to cadaveric specimens and anonymized patient's datasets, so that there is no risk of identification.

Informed consent Consent was not obtained given that presented data corresponding to patient's datasets are anonymized and there is no risk of identification.

References

1. Hassoun-Turkmani A, AL. D (2016) Microsurgery of paraclinoid aneurysms. In: Youmans W (ed) Neurological surgery, vol 4, 7th edn, pp 3298–3306
2. Akabane A, Saito K, Suzuki Y, Shibuya M, Sugita K (1995) Monitoring visual evoked potentials during retraction of the canine optic nerve: protective effect of unroofing the optic canal. J Neurosurg 82:284–287. https://doi.org/10.3171/jns.1995.82.2.0284
3. Boari N, Spina A, Giudice L, Gorgoni F, Bailo M, Mortini P (2017) Fronto-orbitozygomatic approach: functional and cosmetic outcomes in a series of 169 patients. J Neurosurg 1–9. https://doi.org/10.3171/2016.9.JNS16622
4. Chang HS, Joko M, Song JS, Ito K, Inoue T, Nakagawa H (2006) Ultrasonic bone curettage for optic canal unroofing and anterior clinoidectomy. Technical note. J Neurosurg 104:621–624. https://doi.org/10.3171/jns.2006.104.4.621
5. Chen S, Kato Y, Kumar A, Sinha R, Oguri D, Oda J, Watabe T, Imizu S, Sano H, Hirose Y (2013) Contralateral approach to unruptured superior hypophyseal artery aneurysms. J Neurol Surg A Cent Eur Neurosurg 74:18–24. https://doi.org/10.1055/s-0032-1326944
6. Clatterbuck RE, Tamargo RJ (2005) Contralateral approaches to multiple cerebral aneurysms. Neurosurgery 57:160–163 discussion 160-163
7. Day AL (1990) Aneurysms of the ophthalmic segment. A clinical and anatomical analysis. J Neurosurg 72:677–691. https://doi.org/10.3171/jns.1990.72.5.0677
8. de Oliveira E, Tedeschi H, Siqueira MG, Ono M, Fretes C, Rhoton AL Jr, Peace DA (1996) Anatomical and technical aspects of the contralateral approach for multiple aneurysms. Acta Neurochir 138:1–11 discussion 11
9. Fries G, Perneczky A, van Lindert E, Bahadori-Mortasawi F (1997) Contralateral and ipsilateral microsurgical approaches to carotid-ophthalmic aneurysms. Neurosurgery 41:333–342 discussion 342-333
10. Gelber BR, Sundt TM Jr (1980) Treatment of intracavernous and giant carotid aneurysms by combined internal carotid ligation and extra- to intracranial bypass. J Neurosurg 52:1–10. https://doi.org/10.3171/jns.1980.52.1.0001
11. Germanwala AV, Hofler R, Lagman C, Chung LK, Khalessi AA, Zada G, Smith ZA, Dahdaleh NS, Bohnen AM, Cho JM, Colen CB, Duckworth E, Kan P, Lam S, Kim CY, Li G, Lim M, Sherman JH, Wang VY, Yang I (2017) Neurosurgery concepts: key perspectives on endoscopic versus microscopic resection for pituitary adenomas, surgical decision-making in tuberculum sellae meningiomas, optic nerve mobilization during resection of craniopharyngiomas, and evaluation of headache and quality of life after endoscopic transphenoidal surgery for pituitary adenomas. Surg Neurol Int 8:52. https://doi.org/10.4103/sni.sni_17_17
12. Gibo H, Lenkey C, Rhoton AL Jr (1981) Microsurgical anatomy of the supraclinoid portion of the internal carotid artery. J Neurosurg 55:560–574. https://doi.org/10.3171/jns.1981.55.4.0560
13. Hongo K, Watanabe N, Matsushima N, Kobayashi S (2001) Contralateral pterional approach to a giant internal carotid-ophthalmic artery aneurysm: technical case report. Neurosurgery 48:955–959
14. Kakizawa Y, Tanaka Y, Orz Y, Iwashita T, Hongo K, Kobayashi S (2000) Parameters for contralateral approach to ophthalmic segment aneurysms of the internal carotid artery. Neurosurgery 47:1130–1137
15. Kang S, Yang Y, Kim T, Kim J (1997) Sudden unilateral blindness after intracranial aneurysm surgery. Acta Neurochir 139:221–226
16. Kobayashi S, Kyoshima K, Gibo H, Hegde SA, Takemae T, Sugita K (1989) Carotid cave aneurysms of the internal carotid artery. J Neurosurg 70:216–221. https://doi.org/10.3171/jns.1989.70.2.0216
17. Kockro RA, Killeen T, Ayyad A, Glaser M, Stadie A, Reisch R, Giese A, Schwandt E (2016) Aneurysm surgery with preoperative three-dimensional planning in a virtual reality environment: technique and outcome analysis. World Neurosurg 96:489–499. https://doi.org/10.1016/j.wneu.2016.08.124
18. McMahon JH, Morgan MK, Dexter MA (2001) The surgical management of contralateral anterior circulation intracranial aneurysms. J Clin Neurosci 8:319–324
19. Nacar OA, Rodriguez-Hernandez A, Ulu MO, Rodriguez-Mena R, Lawton MT (2014) Bilateral ophthalmic segment aneurysm clipping with one craniotomy: operative technique and results. Turk Neurosurg 24:937–945. https://doi.org/10.5137/1019-5149.JTN.12586-14.1
20. Nakao S, Kikuchi H, Takahashi N (1981) Successful clipping of carotid-ophthalmic aneurysms through a contralateral pterional approach: report of two cases. J Neurosurg 54:532–536
21. Nishio S, Matsushima T, Fukui M, Sawada K, Kitamura K (1985) Microsurgical anatomy around the origin of the ophthalmic artery with reference to contralateral pterional surgical approach to the carotid-ophthalmic aneurysm. Acta Neurochir 76:82–89
22. Oikawa S, Kyoshima K, Kobayashi S (1998) Surgical anatomy of the juxta-dural ring area. J Neurosurg 89:250–254. https://doi.org/10.3171/jns.1998.89.2.0250
23. Oshiro EM, Rini DA, Tamargo RJ (1997) Contralateral approaches to bilateral cerebral aneurysms: a microsurgical anatomical study. J Neurosurg 87:163–169. https://doi.org/10.3171/jns.1997.87.2.0163
24. Renn WH, Rhoton AL Jr (1975) Microsurgical anatomy of the sellar region. J Neurosurg 43:288–298. https://doi.org/10.3171/jns.1975.43.3.0288
25. Rhoton AI Jr (2002) Cranial anatomy and surgical approaches. Neurosurgery 53:1–746
26. Rizzo JF 3rd (1995) Visual loss after neurosurgical repair of paraclinoid aneurysms. Ophthalmology 102:905–910

27. Rozen WM, Chubb D, Stella DL, Taylor GI, Ashton MW (2009) Evaluating anatomical research in surgery: a prospective comparison of cadaveric and living anatomical studies of the abdominal wall. ANZ J Surg 79:913–917. https://doi.org/10.1111/j.1445-2197.2009.05143.x
28. Serrano LE, Ayyad A, Archavlis E, Schwandt E, Nimer A, Ringel F, Kantelhardt SR (2018) A literature review concerning contralateral approaches to paraclinoid internal carotid artery aneurysms. Neurosurg Rev. https://doi.org/10.1007/s10143-018-01063-3
29. Shiokawa Y, Aoki N, Saito I, Mizutani H (1988) Combined contralateral pterional and interhemispheric approach to a subchiasmal carotid-ophthalmic aneurysm. Acta Neurochir 93:154–158
30. Vajda J, Juhasz J, Pasztor E, Nyary I (1988) Contralateral approach to bilateral and ophthalmic aneurysms. Neurosurgery 22:662–668
31. van Lindert E, Perneczky A, Fries G, Pierangeli E (1998) The supraorbital keyhole approach to supratentorial aneurysms: concept and technique. Surg Neurol 49:481–489 discussion 489-490
32. Yamada K, Hayakawa T, Oku Y, Ushio Y, Yoshimine T, Kawai R (1984) Contralateral pterional approach for carotid-ophthalmic aneurysm: usefulness of high resolution metrizamide or blood computed tomographic cisternography. Neurosurgery 15:5–8
33. Yaşargil MG (1984) Clinical considerations, surgery of the intracranial aneurysms and results, vol 2. Thieme
34. Zimmerman CF, Van Patten PD, Golnik KC, Kopitnik TA Jr, Anand R (1995) Orbital infarction syndrome after surgery for intracranial aneurysms. Ophthalmology 102:594–598

Comments

The authors are to be congratulated for their meticulous work in studying the exposures that can be achieved through the interoptic triangle from the surgeons' perspective. The study is performed on 8 cadaveric specimens as well as 10 clinical datasets using a 3D virtual reality system. The exposure of the contralateral ophthalmic segment of the carotid, the ophthalmic artery, as well as the superior hypophyseal artery is studied, evaluating the relative area exposed with a variety of surgical manipulations like ipsilateral clinoidectomy, drilling of the tuberculum or planum, and contralateral optic nerve mobilization. The study does not necessarily offer something radical, but there are subtle novelties that may make it a worthwhile addition to the literature.

Georgios A. Zenonos
Jacques J. Morcos
FL,USA

In this article, the authors describe the "relative interoptic triangle" (rIOT) and how size of the rIOT influences access to the contralateral ICA, OphA, SHA, and perforators. Eight cadavers and 10 clinical datasets using a 3D-VR system were used. The authors found that a larger rIOT correlated with greater exposure of the contralateral ICA, OphA, SHA, and perforators, which makes logical sense. This concept is demonstrated in Fig. 1, which shows how the surgical approaches alters rIOT size and, therefore, influences visualization of contralateral vascular structures. Figure 4 also demonstrates that significant anterior skull base removal and optic nerve mobilization greatly increase rIOT.

The ideal approach to proximal ICA pathology (i.e., aneurysm) is rarely, if ever, a contralateral approach. If a patient has bilateral ICA aneurysms, the side of approach is that of the more concerning aneurysm, and the look contralaterally is only to assess clip feasibility of the aneurysm to spare the patient a second craniotomy. While the rIOT is influenced by the craniotomy of choice, it also changes with each move of the microscope. Therefore, surgeons can increase or decrease visibility of contralateral lesions by changing their working angle. It is not clear how preoperative assessment and determination of rIOT from a specific working angle would influence intra-operative decisions to look contralaterally or not. In addition, surgeons will only clip contralateral ICA aneurysms if they can safely do so and this is something that can only be determined at surgery.

Fady Charbel
Illinois, USA